RP Materials: Proceedings
Vol. 1, Part 1 (2022) pp. 17–21
e-ISSN:

Cite this article: J. Singh, Simplified model to derive the statistics of photon propagation through an optical coupler and an optical fibre, *RP Materials: Proceedings* Vol. 1, Part 1 (2022) pp. 17–21.

Original Research Article

Simplified model to derive the statistics of photon propagation through an optical coupler and an optical fibre

Jaivir Singh
Department of Physics, J.V.M.G.R.R. College, Charkhi Dadri - 127306, Haryana, India
*Corresponding author, E-mail: jaivir.bmu@gmail.com
Selection and Peer-Review under responsibility of the Scientific Committee of the National Conference on Advanced Engineering Materials (NCAEM 2022).

ARTICLE HISTORY
Received: 13 Aug. 2022
Revised: 12 Nov. 2022
Accepted: 14 Nov. 2022
Published online: 27 Dec. 2022

KEYWORDS
Photon statistics; cascade beam splitter model; optical fiber.

ABSTRACT
To determine the statistics of photon propagation through an optical coupler and an optical fibre, we offer a straightforward model. It is assumed that the coupler is lossless and wavelength independent. We determine the coupler powered by quantum light's transfer matrix. A cascade of beam splitters is used to simulate attenuation in a fibre. We demonstrate that the average photon number decays exponentially with distance for a noiseless and lossy optical fibre. We add a random phase factor to the outputs of the beam splitter to an existing model. This mimics the impact of a fiber's dispersion centre. A photon's time of arrival (TOA) will jitter as a result of scattering.

1. Introduction

We analyse the statistics of an optical coupler and fibre driven by a quantum light source using the continuous mode formalism of light [1, 2]. Quantum light is defined as light in which the average number of photons is so tiny that quantum effects are irreversible [3, 4]. Single photon sources (SPS) and weak laser pulse sources are examples (FLPS). SPS and FLPS are utilised in a variety of quantum optics investigations, including the production of squeezed states [6], Schrodinger cat states [7], and quantum key distribution [5].

2. Quantum beam splitter

Figure 1(a) depicts an abstract model of a linear, four-port lossless QBS [8–11]. Two radiation modes enter the apparatus, interact, and then leave. Anihilation and creation operators are used to characterise the quantized light modes [12]. $a_0(\omega)$ and $a_1(\omega)$ stand in for the input operators. The following operators are compliant with the canonical commutation rules [8, 9]:

$$[a_i(\omega), a_j^\dagger(\omega')] = \delta_{ij}(\omega-\omega') \tag{1}$$

The output operators are indicated by the symbols $a_2^1(\omega)$ and $a_3^1(\omega)$. The output operators' superscripts serve as a gentle reminder that the beam splitter is a single stage. We will eventually need to cascade beam splitters, so this notation will come in handy. A transfer matrix, B, links the input and output operators [8, 9]:

$$\begin{pmatrix} a_2^1 \\ a_3^1 \end{pmatrix} = \begin{bmatrix} T(\omega) & R(\omega) \\ R(\omega) & T(\omega) \end{bmatrix} \begin{pmatrix} a_0 \\ a_1 \end{pmatrix} = B \begin{pmatrix} a_0 \\ a_1 \end{pmatrix} \tag{2}$$

where, T and R are transmission and reflection coefficients. By enforcing the conservation of photon numbers and mandating that input and output operators commute, the matrix members are identified. Assumed by the commutation of operators, measurements at one port can be taken without affecting those at other ports. The prerequisites are met if:

$$|T|^2 + |R|^2 = 1 \text{ and } T^*R + R^*T = 0. \tag{3}$$

3. Photon statistics of optical coupler

An optical coupler is a four port device with two input ports and two output ports used in optical communication to combine or divide light beams [13]. According to the electric fields at the inputs, E_{i1} and E_{i2}, the electric fields at the outputs, E_{01} and E_{02} are stated as follows:

$$\begin{pmatrix} E_{01} \\ E_{02} \end{pmatrix} = \begin{bmatrix} \cos kz & j\sin kz \\ j\sin kz & \cos kz \end{bmatrix} \begin{pmatrix} E_{i1} \\ E_{i2} \end{pmatrix}. \tag{4}$$

where k is the coupling coefficient between input modes. The device's geometry, the distance between the ports, and the radiation modes' propagation constants all influence the coefficient k [14]. The measured power at ports 2 and 3 when a light with power P_{in} is incident on port 0 is $P_{in}\sin^2(kz)$ and P_{in}

$\sin^2(kz)$, respectively. We refer to this as the coupler split ratio $\gamma = \cos^2(kz)$.

We will use an abstract model of the coupler as a cascade of QBS, as shown in Figure 1, to construct the quantum equivalent of equation (4). (b). The n_{th} QBS's output is given by

$$\begin{pmatrix} a_2^n \\ a_3^n \end{pmatrix} = \prod_{i=1}^{i=n} \begin{bmatrix} T & jR \\ jR & T \end{bmatrix} \begin{pmatrix} a_0 \\ a_1 \end{pmatrix} = \begin{bmatrix} T & jR \\ jR & T \end{bmatrix}^n \begin{pmatrix} a_0 \\ a_1 \end{pmatrix}. \quad (5)$$

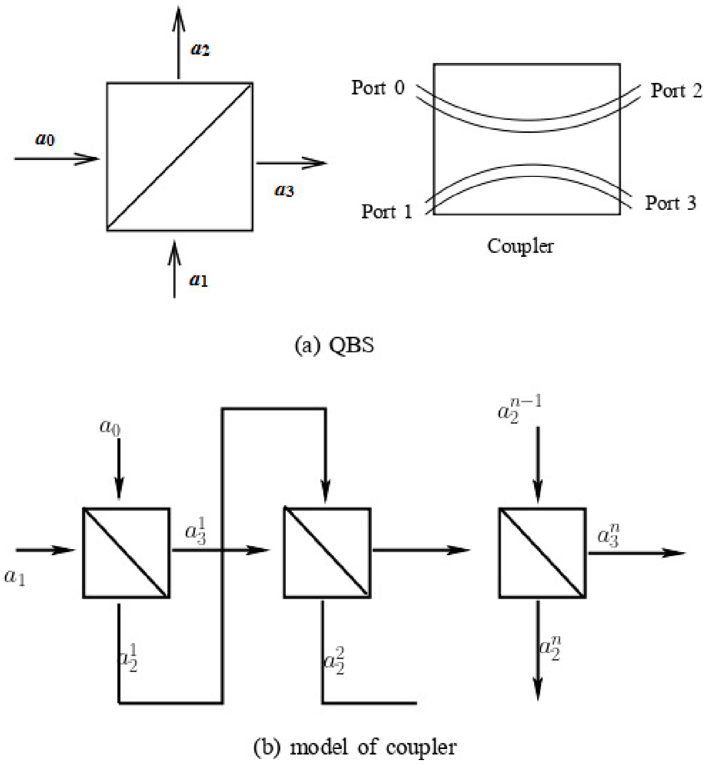

Figure 1: (a) Schematic of quantum beam splitter, (b) Beam splitter model of tap coupler.

By using similarity transformation, the matrix B^n is made simpler, where U and Σ are the unitary and diagonal matrices that are created from the eigenvectors and eigenvalues of B [15]. B's eigenvalues and eigen vectors are $(T \pm jR)$ and $\frac{1}{\sqrt{2}}[\pm 1, 1]^T$, with T standing for transposition in the superscript. Thus, U and Σ become

$$U = \frac{1}{\sqrt{2}} \begin{bmatrix} 1 & -1 \\ 1 & 1 \end{bmatrix} \text{ and } \Sigma = \begin{bmatrix} T + jR & 0 \\ 0 & T - jR \end{bmatrix}. \quad (6)$$

The matrix is generated by substituting equation (6) in equation (5) as:

$$\begin{pmatrix} a_2^n \\ a_3^n \end{pmatrix} = U \begin{bmatrix} (T + jR)^n & 0 \\ 0 & (T - jR)^n \end{bmatrix} U^H \begin{pmatrix} a_0 \\ a_1 \end{pmatrix}. \quad (7)$$

T and R could be one option to satisfy equation (3), along with $R = \sin(k\Delta z)$ and $T = \cos(k\Delta z)$. Energy conservation is ensured by the identification $T^2 + R^2 = 1$ for little $\Delta z, T \approx 1$ and $R \approx k\Delta z$. We permitted $n \to \infty$ and $n\Delta z \to z$. Equation (7) is made simpler by these changes, and the transfer matrix changes to:

$$\begin{pmatrix} a_2(z) \\ a_3(z) \end{pmatrix} = \begin{pmatrix} \cos kz & j\sin kz \\ j\sin kz & \cos kz \end{pmatrix} \begin{pmatrix} a_0 \\ a_1 \end{pmatrix}. \quad (8)$$

We deduce from the transfer matrix that a single photon striking port 0 is detected with probabilities of $\cos^2(kz)$ and $\cos^2(kz)$, respectively, at ports 2 or 3. As a result, the split ratio of a classical coupler is now a gauge of photon detection probability. The average energy measured at ports 2 and 3 approaches γP_{in} and $(1-\gamma)P_{in}$ replicates the traditional result if we repeatedly run the method.

4. Attenuation in optical fiber

A lossy QBS is created by cascading two lossless QBS. As depicted in Figure 2, the lossy QBS are cascaded to represent fibre attenuation. A single stage lossy beam splitter's output is given by

$$\begin{pmatrix} a_2^1 \\ a_3^1 \end{pmatrix} = \begin{pmatrix} T^2 - R^2 & 0 \\ 0 & T^2 - R^2 \end{pmatrix} \begin{pmatrix} a_0 \\ a_1 \end{pmatrix}. \quad (9)$$

The fibre is separated into n parts, each of length $\Delta z = z/n$. The output operators of the n^{th} stage QBS are obtained by repeatedly solving equation (9) as:

$$\begin{pmatrix} a_2^n \\ a_3^n \end{pmatrix} = \begin{pmatrix} (1-2R^2)^n & 0 \\ 0 & (1-2R^2)^n \end{pmatrix} \begin{pmatrix} a_0 \\ a_1 \end{pmatrix}. \quad (10)$$

where $R^2 = \alpha \Delta z$. The fibre attenuation constant, given in neper/m, is shown below. The matrix elements turn into $(1-2R^2)^n \to (1-\alpha\Delta z)^n \simeq \exp(-\alpha z)$ in the limit of big n. Hence, the transfer matrix is provided by

$$\begin{pmatrix} a_2^n \\ a_3^n \end{pmatrix} = \begin{pmatrix} \exp(-\alpha z) & 0 \\ 0 & \exp(-\alpha z) \end{pmatrix} \begin{pmatrix} a_0 \\ a_1 \end{pmatrix}. \quad (11)$$

The input is applied to port 0 and the output is taken from port 2 to make the model resemble an optical fibre. Although port 3 is ignored, port 1 is bound to the vacuum state, which corresponds to no photon injection.

The power measured along the fibre is equal to $P_{in}\exp(-\alpha z)$ when conventional light with a power of P_{in} is transmitted through it. A single photon travelling through the fibre is probabilistically $\exp(-\alpha L)$ detected at $z = L$, according to equation (11). The average power measured approaches $P_{in}\exp(-\alpha L)$ when the process is carried out frequently. When an SPS is used, the quantum attenuation of fibre is calculated as $1 - P_e$, where P_e is the probability of detection ($= \exp(-\alpha z)$).

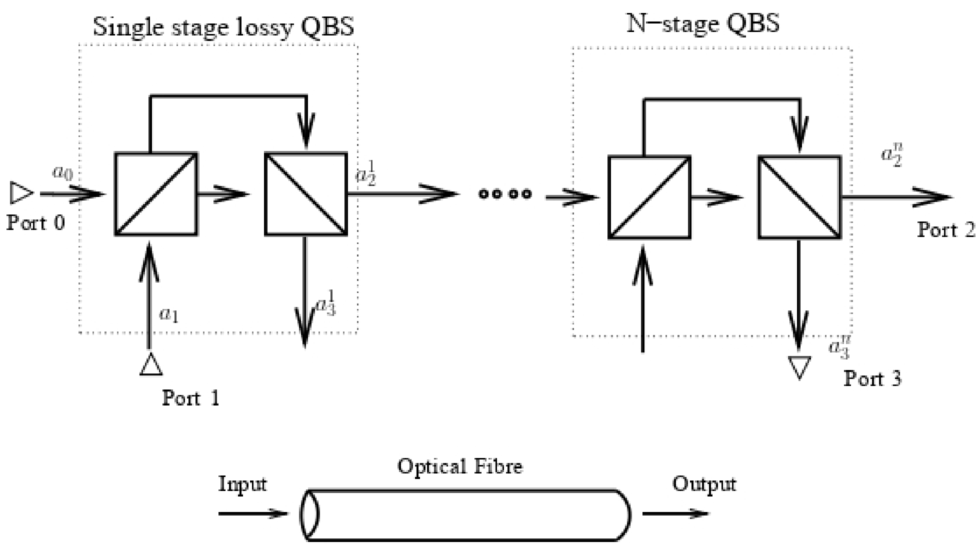

Figure 2: Beam splitters in a cascade are used to simulate noiseless optical fibre attenuation.

4. Effect of scattering centers on photon statistics

The model discussed in the preceding section does not take into account thermal noise or the impact of scattering centres found in a fibre. As shown below, we expand the model to account for these effects.

A. Effect of thermal noise

The thermal noise associated with a radiation mode of frequency ω provided at absolute temperature T is given by $\hbar\omega/[\exp(\hbar\omega/kT)-1]$ [16], which is denoted by operators $\{a_m(z,\beta),\ m = 1,2,3,...\}$. Noise in various modes β_m and β_n , at various locations, and z and z' are all uncorrelated. The following commutation rules [1] are satisfied by thermal noise operators:

$$[a_m(z), a_k^\dagger(z')] = \delta_{km}(\Delta z)^{1/2}\delta(z-z')\delta(\omega-\omega') . \quad (12)$$

Consider the noisy optical fibre represented by the QBS cascade in Figure 3. Noise is dispersed along the fibre as the signal enters the port a_{in} . The output operator a_{out} can be found by using [1].

$$a_{out}(z) = \exp(-\alpha z)a_{in}(z)$$
$$+ j\sqrt{2\alpha(\omega)}\int_0^z dz'\exp[-\alpha(z-z')a_m(\omega,z') . \quad (13)$$

B. Effect of scattering

The scattering centre in a fibre adds a second random phase to the incident light modes' phase. Structure flaws, contaminants, and trapping centres all contribute to the formation of these centres. By altering the model in Figure 3, we can evaluate the impact of the scatterer. By adding random phase φ_i^T and φ_i^R to the transmitted and reflected beams of i^{th} beam splitter, the scatter induced phase is mimicked. By repeatedly evaluating equation (2) as follows:

$$a_{out}^n = T^n \exp[j(\Sigma_n \varphi_n^T)]a_{in}$$
$$+ jR\sum_{m=1}^{n} T^{n-m}\exp(j\varphi_m^R)\exp[j(\Sigma_m \varphi_m^T)]a_m . \quad (14)$$

We define $\varphi^T = \lim_{n\to\infty}\sum_{m=1}^{n}\varphi_m^T$. From equation (3), we see that the sum φ^T and φ^R is equal to π , i.e, $\varphi^T + \varphi^R = \pi$. The output operator is now given by

$$a_{out}(z) = \exp(-\alpha z)\exp[j\varphi^T(z)]a_{in}(z)$$
$$+ j\sqrt{2\alpha(\omega)}\exp[j\varphi^T(z)]$$

$$\times\int_0^z dz'\exp[-\alpha(z-z')\exp[j\varphi^R(z')]a_m(\omega,z') \quad (15)$$

φ_i^T and φ_i^R are independent and identically distributed random variables with uniform distribution over $[0,\pi]$ with mean $\pi/2$ and $\pi^3/24$. By central limit theorem [17], the phase φ^T is Gaussian distributed with mean and variance of the constituent random variables.

C. Single photon input

Let a single photon of frequency ω_0 emitted at time $t = t_0$ be input to the fibre. The operator representing the photon is given by

$$a_{in}(t, z=0) = \exp(-j\omega_0 t_0)\delta(t-t_0)$$

or

$$a_{in}(\omega, z=0) = \exp[-j(\omega-\omega_0)t_0]\,. \quad (16)$$

The attenuation of the fibre is α_0. The wave vector k is expanded around $\omega=\omega_0$ using Taylor series and keeping only the first two terms

$$k = k_0 + (\omega-\omega_0)k'$$

The output operator, $a_{out}(\omega, z)$ is given by

$$a_{out}(\omega,z) = \exp(-\alpha_0 z).\exp(jk_0 z)$$
$$\times\exp[j\varphi_T(z)].\exp[-j(\omega-\omega_0)(t-k'z)]\,. \quad (17)$$

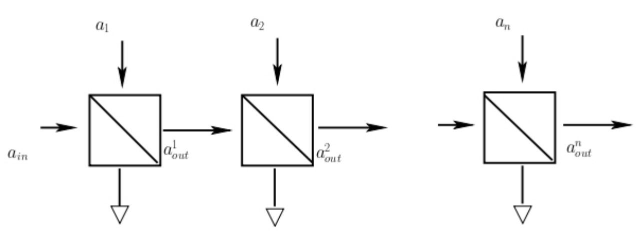

Figure 3: Cascade of beam splitter to model attenuation in fibre including thermal noise.

By taking Fourier transform of equation (17), we get

$$a_{out}(t,z) = \exp(-\alpha_0 z).\exp[j\varphi_T(z)].\exp(jk_0 z).\delta(t-t_0-k'z) \quad (18)$$

Equation (18) reveals that a photon moves through a fibre at a velocity of $1/k'$. The photon is probabilistically $\exp(-\alpha_0 z)$ detected by a detector positioned at z. However, the detection is accompanied by a jitter in the photon's time of arrival (TOA), which is caused by the unpredictable phase angle φ^T. When creating single photon detectors for use in applications like range finding, which depend on TOA photon measurement to determine target range, the jitter is important.

D. Coherent state input

The output amplitude is changed into $\beta\exp[-j\varphi_T(z)]$ if a coherent state [11] with a complex amplitude β is fed into a noiseless optical fibre. Despite the fact that the average number of photons $|\beta|^2$ has not changed, the phase shift of the coherent state upon reflection has changed to a random variable $\pi/2$. The average photon quantity across a specific cross section of fibre is uncertain by the amount of variance of due to the uncertainty in phase φ^T, i.e. $\pi^2/12$. The number phase uncertainty relation [11] predicts this.

5. Conclusions

To determine photon statistics in two optical devices—a coupler and an optical fiber—we combined an abstract model for QBS with the continuous mode formalism of light. We were able to obtain the quantum equivalent of a coupler's SPS-driven transfer matrix. We demonstrated that in an attenuating medium, such as optical fibre, the average photon quantity decreases exponentially with distance. We expanded the model to take into account the impact of fibre scattering centres on individual photons and coherent states.

References

[1] J.R. Jeffers, N. Imoto, R. Loudon., Quantum optics of traveling-wave attenuators and amplifiers, *Phys. Rev. A* **47** (1993) 3346-3350.

[2] K.J. Blow, R.Loudon, S.J.D. Phoenix, T.J. Shepherd, Continuum fields in quantum optics, *Phys. Rev. A*, **42** (1990) 4102-4114.

[3] J. Brendel, E. Mohler, W. Martienssen, Experimental test of Bell's inequality for energy and time, *Europhys. Lett.* **20** (1992) 575-580.

[4] R. Lange, J. Brendel, E. Mohler, W. Martiensen, Beam splitting experiments with classical and with quantum particles, *Europhys. Lett.* **5** (1988) 619-624.

[5] O.L. Guerreau, Long distance QKD transmission using single sideband detection scheme with WDM synchronization, *IEEE J. Quant. Electron.* **9** (2003) 1533-1540.

[6] M. Bloch, S.W. McLaughlin, J.M. Merolla, F. Patois, Frequency-coded quantum key distribution, *Opt. Lett.* **32** (2007) 301-303.

[7] W. Schleich, M. Pernigo, F. Le Kien, Nonclassical state from two pseudoclassical states, *Phys. Rev. A* **44** (1991) 2172-2178.

[8] U. Leonhardt, Quantum statistics of a lossless beam splitter: SU(2) symmetry in phase space, *Phys. Rev. A* **48** (1993) 3265-3270.

[9] R.A. Campos, B.E.A. Saleh, M.C. Teich, Quantum-mechanical lossless beam splitter: SU(2) symmetry and photon statistics, *Phys. Rev. A* **40** (1989) 1371-1384.

[10] J. Schwinger, *On angular momentum*, U.S. At. Energy Commun. (1952). Reprinted in *Quantum Theory of Angular Momentum*, L.C. Biedenharn, H.V. Dam (Ed.), Academic press, New York (1965).

[11] C.C. Gerry, P. Knight, Beam splitters and interferometers, in *Introductory quantum optics*, Cambridge University Press, London (2005).

[12] L. Mandel, E. Wolf, *Optical Coherence and Quantum Optics*, Cambridge University Press, London (1995).

[13] R. Ramaswamy, K. Sivarajan, *Optical networks*, Morgan Kaufmann Pub. (2002).

[14] A. Yariv, *Optical Electronics in Modern Communication*, Oxford University Press, London (1997).

[15] G. Strang, Eigenvalues and Eigenvectors, in *Linear*

Algebra and its Applications, Thomson-Brookscole (1998).
[16] H.A. Haus, *Electromagnetic Noise and Quantum Optical Measurements*, Springer-Verlag, Berlin (2000).
[17] J.G. Proakis, *Digital Communication*, McGraw Hill Pub, New Delhi (2000).
[18] G.P. Agrawal, *Fiber Optic Communication Systems*, John Wiley, New York (1997).
[19] P.A.M. Dirac, *The Principles of Quantum Mechanics*, Oxford University Press, London (1958).